Journal of Thermal Analysis and Calorimetry, Vol. 96 (2009) 1, 321–330

ROLE OF VAPOUR OVERSATURATION IN THE THERMAL DECOMPOSITION OF SOLIDS

B. V. L'vov[*]

Department of Analytical Chemistry, St. Petersburg State Polytechnical University, St. Petersburg 195251, Russia

Elementary thermochemical calculations show that in all cases of formation of solid product in the process of the congruent dissociative vaporization of reactants, the equilibrium partial pressure of the main product greatly exceeds its saturation vapour pressure, and therefore causes the appearance of vapour oversaturation. The oversaturation is responsible for the formation and growth of nuclei, their shape and position, the transfer of condensation energy to the reactant, the existence of induction and acceleration decomposition periods, the reaction localization, the epitaxial/topotaxy effects and the nanocrystal structure of the solid product. Variations in the energy transfer explain an increase of the molar enthalpy with temperature and the decelerating influence of melting on the rate of decomposition.

Keywords: *enthalpy vs. melting, enthalpy vs. temperature, induction and acceleration, nucleation, product structure, reaction localization*

Introduction

Vapour oversaturation (or supersaturation) is a well-known phenomenon, responsible for many natural and industrial processes, related to the formation of mists and clouds, volcanic ashes, industrial (e.g., welding) fumes and smokes, and the use of chemical vapour decomposition technologies in the production of new materials [1–5]. Common to all these different phenomena is the process of vapour condensation with the formation of the new liquid/solid phase. No wonder that some prominent scientists in solid-state kinetics (Volmer, Schwab, Roginsky, Zawadzki and Bretsnajder) attempted to relate this phenomenon to the nucleation and growth of solid product in the process of solid-state decomposition many decades ago. In particular, Prof. Zawadzki took part in a general discussion 'Chemical reactions involving solids' held by the Faraday Society at the University of Bristol in April 1938. (Professors Bernal, Garner, Polanyi, Wagner and other well-known scientists participated in this meeting.) The Report of this meeting, including all the papers contributed, together with the discussion thereon, appeared in the Transactions of the Faraday Society [6, 7].

As it has been clearly emphasized by Zawadzki in the course of that general discussion: 'Supersaturation is a necessary condition for the formation of nuclei… Supersaturation is also essential when already existing crystallites grow via the stages of plane nuclei…' However, to use this phenomenon in the present context, it was necessary to explain the origin of vapour supersaturation in the process of solid decomposition. Zawadzki and Bretsnajder proposed the following explanation for the appearance of supersaturation [6]: 'Our attempts at elucidating this phenomenon were based on the facts that the vapour pressure of liquids and solids varies with the particle size, and the crystallization of solutions yields large, well-developed crystals, or aggregates of small, agglomerated crystals, according to the degree of supersaturation of the solutions… We made use, for interpreting these spurious equilibriums, of models of systems consisting of crystals of different sizes, and assumed that the dissociation pressure of very finely divided $CaCO_3$ must exceed that of large crystals…'.

The decisive role of supersaturation in solid-state decomposition reactions was supported by Roginsky. In his paper 'On the role of supersaturation and on the limiting stage in topochemical reactions', Roginsky [7] wrote: 'As an illustration of the influence of supersaturation on the character of the kinetical equation, consider the simple topochemical kinetics of the dehydration of crystal hydrates and of the decomposition of carbonates… To simplify the theoretical analysis we shall examine only the cases of monocrystals, and of powders consisting of crystals of the same type and the same size… Deviation from equilibrium may occur because of the incipient evaporation of a plane film from the edges and tops (rather than from the face)… In particular, there must be mentioned the interesting series of articles of Zawadzki and Bretsnajder. These authors having expressed opinions very near those mentioned above…'.

It is interesting that during the analysis of the origin of vapour supersaturation, Zawadzki and Bretsnajder considered some other hypotheses, which

* borislvov@rambler.ru

1388–6150/$20.00

Akadémiai Kiadó, Budapest, Hungary
Springer, Dordrecht, The Netherlands

in their opinion, were far from reality: 'It is known with certainty that the reaction $CaCO_3$=CaO+CO_2 does not involve volatilization of $CaCO_3$, followed by dissociation in the vapour phase to CO_2 and CaO, which then crystallizes; the actual reaction velocity is very many times greater than could correspond with this mechanism. It might be supposed that whilst $CaCO_3$ molecules do not actually enter into the gaseous phase, yet they may escape from the space lattice… Here they may move freely, as described by Volmer, and may dissociate, after which the CaO produced would enter an appropriate place on the surface of a growing CaO crystal… We do not, however, think that the above representation corresponds to the actual conditions, as such a mechanism would be in conflict with the topochemical nature of the process, with the results of pseudomorph formation, and with a number of other facts' [6]. (As is now apparent, this representation, based on the volatilization and dissociation of $CaCO_3$ and crystallization of CaO, was very close to reality.)

This surge of interest to the problem of supersaturation in the decomposition kinetics has been superseded by full oblivion [8–10]. The problem was practically forgotten for a long time. It has become evident that within the framework of the incongruent mechanism of decomposition the explanation of vapour supersaturation through the difference in the size of particles was not applicable to single crystals, and that the differences in vaporization rates of atoms/molecules from different sites of the crystal surface are not enough to support the high degree of vapour supersaturation.

Only 60 years afterwards, the author of the present work addressed the given problem again within the framework of the mechanism of congruent dissociative vaporization (CDV). Two citations can be given. 'It should be pointed out that the mechanism of congruent dissociative vaporization with simultaneous condensation of the low-volatile product at the reactant/product interface provides a straightforward explanation for a number of features in the solid-state decomposition process, which have not yet found convincing interpretation. Among them is the mechanism of nucleation through condensation of supersaturated vapour of the low-volatile product…' [11]. 'We believe that many of the kinetic features of the process which still have not found convincing interpretation… can find a simple explanation within the mechanism of dissociative evaporation, if one takes into account the stage of condensation of the non-volatile component from oversaturated vapour and partial transfer of condensation energy from the product to the reactant' [12].

The purpose of this work is, firstly, to estimate the value of vapour oversaturation in the process of solid-state decomposition for several typical classes of reactants and, secondly, to discuss the impact of vapour oversaturation on some peculiarities of these reactions. In the process of this discussion, the azthor will use mainly the material presented in his recently published monograph [13]

Results and discussion

Thermochemical evaluation of vapour oversaturation

One of the essential conditions for the CDV mechanism for reactions ending in the formation of solid products is the presence of the oversaturated vapour of these products above the reactant surface. This becomes obvious when we compare the equilibrium vapour pressure P_{eqp} for the product species at the primary stage of the CDV reaction (disregarding the condensation stage) with the saturated vapour pressure P_{sat}(A) for the solid product A. Table 1 illustrates this reasoning with the corresponding data calculated for some well-known decomposition reactions. These 30 reactions are presented in order of increasing ν/a ratio, and in order of increasing temperature for each ν/a ratio, where ν is the number of moles of all products and a is the number of moles of low-volatile products. An analysis of the data listed in Table 1 yields the following conclusions.

- Contrary to the prevalent opinion, the equilibrium pressure of low-volatility products at the primary stage of the CDV reactions for all compounds is actually much higher than the saturated pressure of these products. For example, the P_{eqp} values of the PbO, CdO and CO_2 species for the decomposition of $PbCO_3$ and $CdCO_3$ at 510 and 573 K are equal to about 10^{-11} bar, which is only two to three orders of magnitude less than the pressure typical for the observable onset of decomposition. At the same time, the saturated pressures for solid PbO and CdO at these temperatures are only $3\cdot10^{-21}$ and $2\cdot10^{-22}$ bar, respectively. One-half the reactants listed in Table 1 begin to decompose at the product vapour pressure in the range of 10^{-9}–10^{-15} bar and one third, in the range of 10^{-9}–10^{-12} bar. The mean value of P_{eqp} is $2\cdot10^{-17}$ bar for all reactants and $1\cdot10^{-13}$ bar for all reactants except the hydroxides and hydrates.
- A general increase of P_{eqp} with the 'dilution' factor (ν/a) is observed. The dilution of the vapour of the low-volatility product with stable gaseous species, in agreement with the thermochemical calculations, increases the equilibrium pressure of this product. For example, the equilibrium pressure of primary

Table 1 Vapour oversaturation of the low-volatility products (P_{eqp}/P_{sat}) in the equimolar mode of CDV (without taking into account the product condensation)

Primary stage of decomposition	ν/*a*	*T*/K	P_{eqp}[a]/bar	P_{sat}(A)[b]/bar	P_{eqp}/P_{sat}
$Ag_2O \leftrightarrow 2Ag(g)+0.5O_2$	1.25	500	$3\cdot10^{-19}$	$6\cdot10^{-24}$	$5\cdot10^{4}$
$LiCl\cdot H_2O \leftrightarrow LiCl(g)+H_2O$	2.0	318	**$3\cdot10^{-15}$**	$2\cdot10^{-28}$	$2\cdot10^{13}$
$BaCl_2\cdot H_2O \leftrightarrow BaCl_2(g)+H_2O$	2.0	333	$1\cdot10^{-25}$	$4\cdot10^{-47}$	$3\cdot10^{21}$
$Li_2SO_4\cdot H_2O \leftrightarrow Li_2SO_4(g)+H_2O$	2.0	350	$7\cdot10^{-25}$	$2\cdot10^{-48}$	$4\cdot10^{23}$
$Cd(OH)_2 \leftrightarrow CdO(g)+H_2O$	2.0	390	$6\cdot10^{-19}$	$6\cdot10^{-37}$	$1\cdot10^{18}$
$Zn(OH)_2 \leftrightarrow ZnO(g)+H_2O$	2.0	400	$4\cdot10^{-25}$	$1\cdot10^{-50}$	$4\cdot10^{25}$
$Be(OH)_2 \leftrightarrow BeO(g)+H_2O$	2.0	400	$5\cdot10^{-35}$	$3\cdot10^{-88}$	$2\cdot10^{53}$
$Mg(OH)_2 \leftrightarrow MgO(g)+H_2O$	2.0	535	$7\cdot10^{-27}$	$2\cdot10^{-53}$	$4\cdot10^{26}$
$Ca(OH)_2 \leftrightarrow CaO(g)+H_2O$	2.0	570	$2\cdot10^{-28}$	$6\cdot10^{-54}$	$3\cdot10^{25}$
$Sr(OH)_2 \leftrightarrow SrO(g)+H_2O$	2.0	590	$4\cdot10^{-24}$	$6\cdot10^{-43}$	$7\cdot10^{18}$
$Ba(OH)_2 \leftrightarrow BaO(g)+H_2O$	2.0	610	$3\cdot10^{-17}$	$2\cdot10^{-28}$	$2\cdot10^{11}$
$PbCO_3 \leftrightarrow PbO(g)+CO_2$	2.0	510	**$2\cdot10^{-11}$**	$3\cdot10^{-21}$	$7\cdot10^{9}$
$CdCO_3 \leftrightarrow CdO(g)+CO_2$	2.0	573	**$1\cdot10^{-11}$**	$2\cdot10^{-22}$	$5\cdot10^{10}$
$ZnCO_3 \leftrightarrow ZnO(g)+CO_2$	2.0	573	**$1\cdot10^{-15}$**	$9\cdot10^{-33}$	$1\cdot10^{17}$
$MgCO_3 \leftrightarrow MgO(g)+CO_2$	2.0	700	$9\cdot10^{-19}$	$2\cdot10^{-38}$	$5\cdot10^{19}$
$CaCO_3 \leftrightarrow CaO(g)+CO_2$	2.0	810	$1\cdot10^{-19}$	$3\cdot10^{-35}$	$3\cdot10^{15}$
$SrCO_3 \leftrightarrow SrO(g)+CO_2$	2.0	900	$4\cdot10^{-17}$	$2\cdot10^{-25}$	$2\cdot10^{8}$
$BaCO_3 \leftrightarrow BaO(g)+CO_2$	2.0	1077	**$5\cdot10^{-9}$**	$5\cdot10^{-13}$	$1\cdot10^{4}$
$Ag_2C_2O_4 \leftrightarrow 2Ag(g)+CO_2+CO+0.5O_2$	2.25	400	**$3\cdot10^{-14}$**	$4\cdot10^{-31}$	$8\cdot10^{16}$
$AgNO_3 \leftrightarrow Ag(g)+NO_2+0.5O_2$	2.5	470	**$1\cdot10^{-12}$**	$1\cdot10^{-25}$	$1\cdot10^{13}$
$BaCl_2\cdot 2H_2O \leftrightarrow BaCl_2(g)+2H_2O$	3.0	333	$3\cdot10^{-23}$	$4\cdot10^{-47}$	$8\cdot10^{23}$
$BeSO_4 \leftrightarrow BeO(g)+SO_2+O$	3.0	875	$3\cdot10^{-17}$	$1\cdot10^{-35}$	$3\cdot10^{18}$
$MgSO_4 \leftrightarrow MgO(g)+SO_2+O$	3.0	1000	$3\cdot10^{-14}$	$3\cdot10^{-24}$	$1\cdot10^{10}$
$NiC_2O_4 \leftrightarrow Ni(g)+CO+CO_2+0.5O_2$	3.5	540	**$9\cdot10^{-14}$**	$2\cdot10^{-34}$	$5\cdot10^{20}$
$PbC_2O_4 \leftrightarrow PbO(g)+2CO+0.5O_2$	3.5	550	**$8\cdot10^{-11}$**	$3\cdot10^{-19}$	$3\cdot10^{8}$
$MnC_2O_4 \leftrightarrow MnO(g)+2CO+0.5O_2$	3.5	610	**$5\cdot10^{-13}$**	$9\cdot10^{-36}$	$6\cdot10^{22}$
$Cd(NO_3)_2 \leftrightarrow CdO(g)+2NO_2+O$	4.0	560	**$3\cdot10^{-11}$**	$4\cdot10^{-23}$	$8\cdot10^{11}$
$Pb(NO_3)_2 \leftrightarrow PbO(g)+2NO_2+O$	4.0	560	**$1\cdot10^{-11}$**	$8\cdot10^{-19}$	$1\cdot10^{7}$
$Ba(N_3)_2 \leftrightarrow Ba(g)+0.74N+2.63N_2$	4.37	400	**$1\cdot10^{-9}$**	$2\cdot10^{-18}$	$5\cdot10^{8}$
$Pb(N_3)_2 \leftrightarrow Pb(g)+2.36N+1.82N_2$	5.18	520	**$1\cdot10^{-9}$**	$1\cdot10^{-14}$	$1\cdot10^{5}$

[a]Magnitudes of $P_{eqp} \geq 10^{-15}$ bar are marked by bold. [b]A: a low-volatility product.

products (Ag, NO_2 and O_2) for the decomposition of $AgNO_3$ is close to 10^{-12} bar. The rise of P_{eqp} value as compared to that for Ag_2O ($3\cdot10^{-19}$ bar) is related to the difference in the ratios ν/*a* for these reactions: 2.5 for $AgNO_3$ and 1.25 for Ag_2O.

- The saturated pressure of solid products in the case of the decomposition of H_2O-containing compounds (hydrates and hydroxides), which is in the range of 10^{-28}–10^{-88} bar as a whole, is much lower than that for other compounds (oxides, carbonates, nitrates, sulfates, oxalates and azides): 10^{-14}–10^{-38} bar. The main reason for this is the difference of the mean decomposition temperatures: 440±100 K for the hydrates and hydroxides compared to 640±200 K for other reactants.
- The correlation between P_{eqp} and P_{sat} values at $\nu/a \geq 2$ and 10^{-18} bar$>P_{sat}>10^{-53}$ bar can be described as follows: $\log P_{eqp}=0.48 \log P_{sat} - 0.9$ (Fig. 1) or approximately, as

$$\log P_{eqp} \cong 0.5 \log P_{sat} \quad (1)$$

The correlation coefficient (*r*) is 0.94 and the standard deviation in units of log P_{eqp} is equal to ±1.9.

- The vapour oversaturation degree, which can be defined as the ratio of the equilibrium partial pressure of a product, P_{eqp}, to the saturated pressure, P_{sat}, of this product:

$$S \equiv P_{eqp}/P_{sat} \quad (2)$$

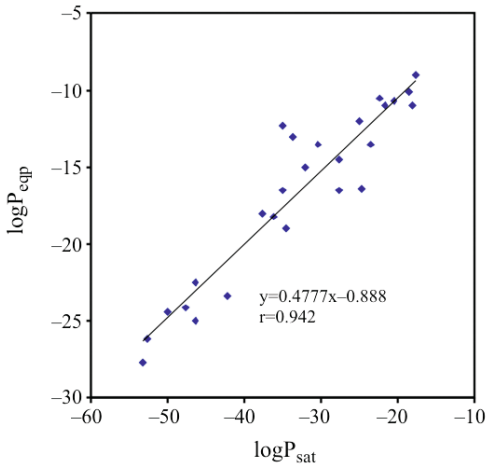

Fig. 1 Correlation between P_{eqp} and P_{sat} values at $\nu/a \geq 2$ and 10^{-18} bar$>P_{sat}>10^{-53}$ bar

varies in the range from 10^3 for Ag_2O to 10^{53} for $Be(OH)_2$ at the primary (induction) stage of the CDV reaction. Taking into account Eq. (1), we obtain at $\nu/a \geq 2$ and 10^{-18} bar$>P_{sat}>10^{-53}$ bar:

$$\log S \cong -0.5 \log P_{sat} \quad (3)$$

The vapour oversaturation degree in the reaction interface (when $P_{eqp} \cong 2 \cdot 10^{-8}$ bar) varies in the range from 10^5 for $BaCO_3$ to 10^{80} for $Be(OH)_2$.

When the equilibrium vapour pressure of the low-volatility products is low, the concentration of atoms or molecules is sometimes as low as a few particles per 1 cm^3 (four atoms of Ag in the Ag_2O decomposition) or even lower. Nevertheless, being in oversaturated concentration, they should condense on the reactant surface with the possible formation of germ nuclei. The value of the equilibrium pressure of the products can be used to interpret some features of this process. For example, from the comparison of P_{eqp} values in Table 1 it may be proposed that the formation of germ nuclei of Ag, in the process of Ag_2O decomposition, is more difficult and takes more time (the longer induction period) than that for $AgNO_3$ decomposition (all other factors being equal).

Formation and growth of nuclei (preliminary remarks)

Nuclei form at specific points of the reactant crystal lattice. These points are located in regions with disordered structure, for instance, where dislocations emerge onto the surface, at vacancies, at interstitial-ion or impurity clusters. At these points of the lattice the molecules of the original substance may not be as fully coordinated as on an ideal (defect-free) surface and this makes them more susceptible to decomposition.

However, a further development of the process, in particular, the transformation of a thermodynamically unstable, germ nucleus into a stable growth nucleus in the framework of this 'disordered structure' concept remains unclear. Jacobs, one of the founders of formal kinetics, admits [10] that 'we have no knowledge of how the first few hundred atoms are added to a nucleus...'. The driving force behind the subsequent growth of nuclei, which occurs at a rate higher than that of their formation, remains unclear as well. The CDV mechanism presents a simple and straightforward explanation for both of these features. The formation and initial growth of germ nuclei are suggested to be driven by condensation on the reactant surface of oversaturated vapour of the low-volatility product, while the accelerated evolution of the growth nuclei is the result of contributions to the enthalpy of nuclei growth due to vapour condensation and the accompanying liberation of heat in the product/reactant interface.

Shape and position of the nucleus

One of the simplest and most convincing arguments for or against the CDV mechanism should be the position of the germ nucleus on the reactant surface. According to the prevailing concept: 'The germ nucleus may be defined as a small particle of the product phase embedded in reactant… The transformation yielding a germ nucleus is usually identified with a change in crystal structure… The product effectively occupies the volume formerly filled with reactant' [14] so that, as it was stated earlier [9], 'the nucleation process involves conversion of a small volume of reactant into a stable particle of product'.

An obvious consequence of the CDV mechanism and of nucleation through condensation of oversaturated vapour of a low-volatility product is that germ nuclei form on the surface rather than inside the reactant. Hence, to substantiate the validity of a mechanism, one has to analyze the results accumulated in the literature on studies of nucleation by optical and scanning electron microscopy. Universally recognized in this area are studies carried out by Garner with followers in the 1930–1960s and Galwey with colleagues in the 1970–1990s, which are summarized partially in monographs [9, 15, 16].

Garner *et al*. [15] obtained many excellent optical microscopic images of the nuclei forming in the course of decomposition of crystalline hydrates of various salts. (Remarkably, the nuclei frequently resemble in shape crystals crystallizing out of oversaturated solution. This could be support for formation of germ nuclei through condensation of oversaturated vapour). For alums [17, 18], the nuclei appear as rounded-off hemispheres with a slight pit at the center and uneven edges. The most important observation is, however,

that 'the nuclei are always formed on the surface, never within the solid phase' [17].

Studies of the barium azide decomposition led Mott [19] to the same conclusion 'that nuclei are probably formed only at surfaces and that they grow outwards'. As a result of material loss, a pit forms on the surface around the nucleus. Formation of a small pit in the upper part of the nucleus is most probably associated with the dynamics of transport and condensation of decomposition products on a hemispherical surface. Galwey *et al*. [18], in full agreement with the above observations [17, 18] and in conflict with the definition of the nucleus given in [9, 14], point out (for the alum decomposition) that 'the first stage is the appearance on the crystal surface of a small mound (ca. 5 μm diameter) with central pitting'. Later Galwey *et al*. [20] have shown that randomly distributed product particles of 0.2–1.0 μm, with rounded corners and sometimes equidimensional, were observed on the original surface of single crystals of $Li_2SO_4{\cdot}H_2O$.

The nuclei formed in the decomposition of potassium permanganate, are spherical, 1–2 μm in diameter [21]. Each nucleus sits in a small pit on the crystal surface and represents a complex aggregate of smaller, ring-shaped crystals. That these nuclei were formed by condensation, is corroborated by the knotty spherical formations, practically identical in shape, that appear in condensation of carbon vapour on the cooler parts of graphite tubes used in electrothermal AAS [22]. Another feature accompanying the nucleation in the decomposition of $KMnO_4$ consists in the formation of a thin layer of the product (0.1–0.2 μm thick) coating uniformly the whole surface of the crystal. At the slightest touch, it breaks up and flakes off. It grows, most probably, under intensive condensation of gaseous products during the reactor cooling (at the end of the treatment period at 500 K). The 'unmodified' (perhaps, amorphous) character of this film is accounted for, as will be shown below, by the high vapour oversaturation at the moment of condensation. Combination of all the above observations leaves no place for doubt that the germ nuclei form on the surface rather than inside the reactant body.

Induction and acceleration stages (qualitative analysis)

Nucleus growth into the reactant is conducted by the reaction localized at the product/reactant interface. Unlike the enthalpy of the decomposition reaction occurring at the free surface in the induction period (in the absence of nuclei), that of the reaction at the interface decreases because of a partial contribution of the energy released in the product condensation in this zone. This gives rise to an increase in the rate of reactant decomposition and the onset of the acceleratory period in the kinetics curve. The acceleration depends on the difference between the above enthalpies, i.e., on the condensation energy contributed to the heat of the pure vaporization process.

There are two types of decomposition reactions for which the stages of induction and acceleration cannot exist in principle. The first type includes those decompositions, which do not produce low-volatility products, and, hence, in which the reaction interface between two solid phases is absent. The second type includes the decompositions of melts, in which such reaction zones cannot form because of the melting of the reactant. Our studies [13] of the decompositions of some oxides (HgO, CdO and ZnO) and nitrides (Mg_3N_2, AlN, GaN, InN and Si_3N_4), which decompose completely to gaseous products, as well as an analysis of literature data, support this conclusion. The kinetics curves of MgH_2, HgO, HgC_2O_4, NH_4IO_3 and NH_4NO_3 were found [9, 15] to satisfy the equation of a contracting sphere. Silver azide, which melts at 523 K [15], and melts of the silver and cadmium nitrates with melting temperatures of 483 and 633 K, respectively, decompose in the same way.

Kinetics curves may often lack, or have barely discernible, induction and acceleration stages, even in the presence of low-volatility products. This can sometimes be achieved by accelerating the slowest stage of the decomposition by creating artificial nuclei of the solid phase by mixing and grinding preliminarily the powders of the reactant and the product (for instance, Ag_2O and Ag [23]). A still more efficient way is to coat Ag_2O particles with a silver film by deposition from metal vapour [23]. With crystalline hydrates, one can reach the same goal by degrading mechanically the surface (for instance, by treating the surface of a single-crystal of $Li_2SO_4{\cdot}H_2O$ with an abrasive [24]).

Reaction localization

The difference between the rates of decomposition from a free surface and at the product/reactant interface accounts for the reaction being localized near the growth nuclei. The higher rate of decomposition at the reaction interface between two solid phases brings about an increase in concentration of molecules (vapour pressure) of the low-volatility product around the nucleus. This favors formation on the surface of new germ nuclei adjoining the original nucleus.

Product structure and the topotaxy effect

A feature frequently observed in the decomposition of crystalline hydrates, which has not yet been given a convincing interpretation in the framework of universally accepted ideas, is the formation of solid products in ei-

ther an amorphous or a crystalline state, depending on the actual water-vapour pressure in the reactor. This phenomenon was observed by Kohlschütter and Nitschmann in 1931 [25] and has been the subject of numerous publications, including the study of Volmer and Seydel [26], who used it as a basis for explaining the Topley–Smith effect, and a series of articles by Frost *et al*. [27–29]. Dehydration of many crystalline hydrates in vacuum entails formation of an X-ray amorphous (finely dispersed) residue and, in the presence of water vapour, formation of a crystalline product. The highest H_2O pressure at which an amorphous product can still form varies for different hydrates from a few tenths to a few Torr. As the decomposition temperature increases, the boundary of formation of the crystalline product shifts toward higher H_2O pressures [28].

Most of the researchers [26–29] attribute this effect to accelerated recrystallization of the dehydrated amorphous product initiated by the presence of water vapour, although the mechanism responsible for this influence is far from being obvious.

It appears much simpler to explain the differences in formation of the X-ray amorphous and crystalline products as due to a change of the real temperature of the crystalline hydrate at the instant of decomposition and the accompanying differences in vapour oversaturation. Although the reactor temperature is maintained constant in experiments on dehydration in the presence of water vapour, the temperatures of the hydrate decomposing in vacuum and in the presence of water vapour may differ by ten or more degrees because of the intense self-cooling of the hydrate.

We assume that the differences in formation of the condensates with different structures (or, to be exact, of crystallites differing in size) are determined by the degree of oversaturation, S, of the vapour of the condensing substance. In connection with this assumption, one can refer to the Gibbs–Thomson equation:

$$\ln S = \frac{2M\gamma}{RT\rho r} \qquad (4)$$

which is valid for drops of a liquid with a molar mass, M, surface tension, γ and density, ρ, in equilibrium with oversaturated vapour. The magnitude of oversaturation can be identified with a certain critical radius, r, of the primary condensation nuclei. The equation shows that the critical radius of particles decreases with increasing oversaturation. This is probably the key to the explanation of the different structure of solid condensates if only Eq. (4) is applicable in this case.

The above-listed features of the formation of X-ray amorphous and crystalline products are also observed in the decompositions at high temperatures. Haul and Schöning [30] applied an X-ray method (line-width technique) to study the structure of the decomposition products of dolomite as a function of temperature. The size of the crystallites formed in vacuum increased monotonically from 6 nm for MgO and 13 nm for CaO to 120–140 nm with the temperature increasing within the range 700–1000°C. (Oversaturation decreases in these conditions from 10^{16} to 10^{8} for MgO, and from 10^{19} to 10^{11} for CaO. Lee *et al*. [31] observed an increase of the size of MgO crystallites from 26 nm at 700°C to 98 nm at 1000°C in the process of calcination of natural magnesite under flowing air (20 mL min^{-1}).

Searcy *et al*. [32–34] observed that the decompositions of magnesium hydroxide and magnesium and barium carbonates obeyed the same relations. The MgO residue obtained after decomposition of $Mg(OH)_2$ and $Mg(CO_3)_2$ (at 540 and 675 K, respectively) was a high-porosity X-ray amorphous product which partially retained (as in epitaxial deposition) the structure of the primary materials. The size of the MgO cubic particles measured by transmission electron microscopy was found to be, accordingly, 2 and 3 nm [32]. In contrast to MgO, the barium oxide obtained in the decomposition of $BaCO_3$ exhibited a clearly pronounced crystalline structure [34]. These differences in structure are compared in Table 2 with the oversaturation magnitudes for MgO and BaO vapour for the decompositions of $Mg(OH)_2$, $MgCO_3$ and $BaCO_3$. The table also contains similar data obtained for $CaCO_3$ and talc ($MgO{\cdot}4SiO_2{\cdot}H_2O$).

As seen from the table, oversaturation turns out to be significantly lower for the $BaCO_3$ decomposition than in all other cases. This accounts for the formation of crystalline BaO rather than amorphous products under these conditions. The above differ-

Table 2 Crystal structure of the product and vapour oversaturation in the process of decomposition of some carbonates and hydroxides [13]

Reactant	Product	Structure	T/K	log$S$[a]	Reference
$BaCO_3$	BaO	crystalline	1080	4.6	[34]
$MgO{\cdot}4SiO_2{\cdot}H_2O$	SiO_2	amorphous	1200	8.2	[13]
$CaCO_3$	CaO	amorphous	800	27.0	[33]
$MgCO_3$	MgO	amorphous	675	31.7	[32]
$Mg(OH)_2$	MgO	amorphous	540	43.9	[32]

[a]At $P_{eqp} \cong 2{\cdot}10^{-8}$ bar.

ences in MgO crystallite size, a factor of 1.5 between $MgCO_3$ and $Mg(OH)_2$, and of 2.0 between $CaMg(CO_3)_2$ [30] and $MgCO_3$ [32], fit the difference in the magnitude of oversaturation. On the whole, the CDV mechanism csn be considered as a theoretical basis of the so/called 'thermolysis technology'widely used in the synthesis of nanocrystals [35].

X-ray diffraction measurements enable also the presence or absence of epitactic and topotactic relationships between reactant and solid product to be established. Such topotactic transformation is characterized by internal atomic displacements in solids, so that the initial and final lattices are in coherence, namely, the product is oriented crystallographically with respect to one or more structural elements of the reactant. This phenomenon has been observed in the cases of decomposition of some carbonates (e.g., $CaCO_3$ and $MgCO_3$), hydroxides, oxides and hydrates [16]. However, the mechanism of these internal atomic displacements in the solid product is not clear. The CDV mechanism with simultaneous condensation of the low-volatile product at the reactant/product interface provides a straightforward explanation for this phenomenon. It is well known that epitaxial vapour condensation is one of the popular methods in modern microelectronics for depositing monocrystalline films on monocrystalline substrates [36].

Impact of vapour condensation on the reaction enthalpy

According to the CDV mechanism, for the decomposition of compound R into gaseous products A and B and the subsequent condensation of the low-volatility component A

$$R(s) \leftrightarrow aA(g) + bB(g) \rightarrow aA(s) + bB(g) \quad (5)$$

an additional term $\tau a\Delta_c H_T^0(A)$ should be introduced into calculation of the decomposition enthalpy. This term takes into account the partial transfer of condensation energy to the reactant. The transfer coefficient, τ, corresponds to the part of the energy $a\Delta_c H_T^0(A)$, returned to the reactant. Thus:

$$\Delta_r H_T^0 = a\Delta_f H_T^0(A) + b\Delta_f H_T^0(B) - \Delta_f H_T^0(R) + \\ + \tau a\Delta_c H_T^0(A) = \Delta_v H_T^0 + \tau a\Delta_c H_T^0(A) \quad (6)$$

where $\Delta_r H_T^0$ and $\Delta_v H_T^0$ are the enthalpies of reaction (5) on the whole and of the initial evaporation process, respectively. Hence, it follows that:

$$\tau = \frac{\Delta_r H_T^0 - \Delta_v H_T^0}{a\Delta_c H_T^0(A)} \quad (7)$$

Originally, the coefficient τ was introduced into the CDV mechanism as an adjustable parameter aimed to connect the *E* parameter with the enthalpy of an assumed reaction [37]. It was supposed [38] that, in the majority of cases, the condensation energy would be distributed equally among solid phases of the reactant and product, so that the coefficient τ would be equal to 0.50. However, as became evident later, when the coefficients τ had been determined for a sufficient number of reactants, this is not true [39].

An analysis of variations of the coefficient τ for 15 different compounds, measured by L'vov and Ugolkov [39–42], allowed these magnitudes to be connected with the oversaturation of the vapour of the low-volatility component at the moment of decomposition. The complete list of these reactants is presented in Table 3.

This dependence, having a correlation coefficient equal to 0.96 can be described by the equation:

Table 3 Dependence of the τ coefficient on the oversaturation degree of low-volatility product at the decomposition temperature

Reactant	Product	T^a/K	P_{sat}/bar	τ	c_1	τ_1	Reference
BN	B	1790	$1.9\cdot10^{-9}$	0.044	1.02	0.020	[36]
$Cd(NO_3)_2$	CdO	563	$5.1\cdot10^{-23}$	0.394	14.6	0.426	[13]
$MgSO_4$	MgO	1000	$2.8\cdot10^{-24}$	0.412	15.9	0.439	[39]
$SrCO_3$	SrO	900	$2.2\cdot10^{-25}$	0.507	17.0	0.449	[13]
$CaCO_3$	CaO	900	$6.7\cdot10^{-31}$	0.449	22.5	0.492	[39]
$Ba(OH)_2$	BaO	600	$6.2\cdot10^{-29}$	0.496	20.5	0.477	[40]
$Cd(OH)_2$	CdO	400	$7.9\cdot10^{-36}$	0.441	27.4	0.522	[40]
$MgCa(CO_3)_2$	MgO+CaO	824	$2.6\cdot10^{-36}$	0.449	27.9	0.524	[41]
$MgCO_3$	MgO	800	$1.6\cdot10^{-32}$	0.536	24.1	0.502	[41]
$Sr(OH)_2$	SrO	600	$6.4\cdot10^{-42}$	0.586	33.5	0.552	[41]
$Zn(OH)_2$	ZnO	400	$9.8\cdot10^{-51}$	0.572	42.3	0.588	[40]
$Mg(OH)_2$	MgO	500	$3.0\cdot10^{-57}$	0.585	48.8	0.610	[40]
$Ca(OH)_2$	CaO	600	$2.1\cdot10^{-50}$	0.632	42.0	0.587	[40]
$Li_2SO_4\cdot H_2O$	Li_2SO_4	300	$4.5\cdot10^{-58}$	0.656	49.6	0.612	[42]
$Be(OH)_2$	BeO	400	$3.4\cdot10^{-88}$	0.724	79.8	0.685	[40]

[a]Temperature that corresponds to $P_{eqp} \cong 2\cdot10^{-8}$ bar.

$$\tau_1=0.351\log c_1+0.017 \quad (8)$$

where $c_1 \equiv \log S$.

The correlation revealed is a very important step in the development and use of CDV mechanism. Firstly, a very unusual relation occurs between the condensation energy transfer (τ coefficient) and vapour oversaturation, *S*, of the low-volatility product. As can be seen from Eq. (8), this relation is doubly logarithmic, and thus, it is very weak. Variation of P_{sat} from $5.1\cdot10^{-23}$ bar for $Cd(NO_3)_2$ to $3.4\cdot10^{-88}$ bar for $Be(OH)_2$ (within 65 orders of magnitude) produces only about a two-fold increase in τ magnitude (from 0.394 to 0.724). The correlation revealed may become a key point in the understanding of the mechanism of condensation energy transfer. (These findings might be of considerable interest to the investigators specialized in the studies of the interaction of high-energy gaseous molecules with solids.)

Secondly, the discovered correlation (in the form of the semi-empirical dependences presented above) may be used for theoretical calculations of decomposition kinetics and for thermochemical analysis of the composition of primary reaction products.

Increase of the reaction enthalpy with temperature

Another consequence of this condensation energy transfer is the enthalpy rise with temperature. The magnitude of oversaturation, which determines the condensation energy transfer to reactant, decreases with a rise in temperature. That is why the contribution of the condensation energy to the enthalpy, owing to the decrease in the τ coefficient (and, to a lesser degree, to the condensation energy itself) should decrease. As a result, instead of the ordinary small decrease of enthalpy with temperature rise, its magnitude should increase.

As an example, Table 4 presents calculated and experimental data for the decomposition of $CaCO_3$. Equation (8) has been used in estimations of the coefficient τ. As can be seen from the table, the temperature rise from 900 to 1200 K is accompanied by an increase in the magnitude of $\Delta_r H_T^0$ by about 50 kJ mol^{-1}, instead of the expected decrease of 10 kJ mol^{-1}. Theoretical results are confirmed quite well by experiments.

It is difficult to overestimate the significance of this effect. First, it provides a convincing proof of the fact of condensation energy transfer to the reactant and supports the validity of the calculations of reaction enthalpies for compounds decomposing with the formation of a low-volatility product. Secondly, it points to the need to revise the main causes of systematic underestimation of results obtained in measurements with the second-law and Arrhenius plot methods [43]. In addition to self-cooling, the condensation effect is also among these causes. Moreover, while the self-cooling effect can be eliminated or reduced by choosing the appropriate experimental conditions, the condensation effect cannot, in principle, be eliminated.

Reactant melting and the decomposition enthalpy

Study of the decomposition rates for solid and liquid (melted) reactants is one more way for verification of the CDV mechanism. Measurements of such kind have been recently described by L'vov and Ugolkov [44] for the decompositions of the anhydrous nitrates of silver and cadmium. Melting temperatures for these salts are equal to 483 and 633 K, respectively. The final results of these experiments are presented in Table 5.

Table 4 Calculated and experimental values of the enthalpy change for the decomposition of $CaCO_3$ [13]

T/K	$\Delta_v H_T^0$/kJ mol^{-1}	$-\Delta_c H_T^0$/kJ mol^{-1}	P_{sat}/bar	c_1[a]	τ_1	$\Delta_r H_T^0$/kJ mol^{-1}	
						theor.[b]	exp.
900	840.6	669.5	$6.7\cdot10^{-31}$	22.5	0.492	511	487±5
1000	837.3	667.8	$5.1\cdot10^{-27}$	18.6	0.463	528	500±7
1100	834.0	666.3	$7.5\cdot10^{-24}$	15.4	0.434	545	515±1
1200	830.0	664.7	$3.2\cdot10^{-21}$	12.8	0.406	561	535±5

[a] $c_1=\log(P_{eqp}/P_{sat})$, where $P_{eqp}\cong2\cdot10^{-8}$ bar. [b] Theoretical results are 25–30 kJ mol^{-1} overstated because of 10% underestimation of τ_1 parameter calculated by approximate Eq. (8).

Table 5 Kinetic parameters for the decomposition of solid and melted nitrates in a vacuum [44]

Nitrate	*T*/K	Primary products	*J*/kg m^{-2} s^{-1}	*E*/kJ mol^{-1}
$AgNO_3(s)$	472	$Ag(g)\downarrow+NO_2+0.5O_2$	$3\cdot10^{-7}$	146.6±0.4
$AgNO_3(l)$	574	$Ag(g)+NO_2+0.5O_2$	$8\cdot10^{-7}$	165.5±0.8
$Cd(NO_3)_2(s)$	563	$CdO(g)\downarrow+2NO_2+O$	$7\cdot10^{-6}$	177.5±1.0
$Cd(NO_3)_2(l)$	660	$CdO(g)+2NO_2+5O$	$9\cdot10^{-6}$	198.1±0.8

As can be seen from Table 5, regardless of the difference in temperatures, the decomposition rates, *J*, for $AgNO_3$ and $Cd(NO_3)_2$ in the solid and molten states appear to be about the same. (With a temperature difference of 100 K, a rate increase by two to three orders of magnitude could be expected.) For some reason the decompositions of the solid reactants slow down after their melting. The magnitude of the molar enthalpy (parameter *E*) rises by about 20 kJ mol^{-1}.

The decelerating influence of melting has a very simple explanation and can be interpreted quantitatively within the framework of the CDV mechanism. A partial transfer of condensation energy ($\tau a \Delta_c H_T^0$) to a solid reactant during the decomposition process causes the decrease of the reaction enthalpy and the increase of the rate. In the absence of such a zone and such a transfer for a molten reactant τ=0, and the reaction enthalpy is higher than that for a solid reactant.

The experimental results for both nitrates agree with the theoretical calculations [13].

The results of similar experiments for $Ca(NO_3)_2$ by Ettarh and Galwey [45] are also in a full agreement with the above approach. The melting point for $Ca(NO_3)_2$ is 836 K. The *E* parameters measured in [45] for solid (774–820 K) and melted nitrate (229±10 and 315±20 kJ mol^{-1}), agree with thermochemical calculations of the molar enthalpy (234 and 318 kJ mol^{-1}) for the corresponding reactions:

$$Ca(NO_3)_2(s) \leftrightarrow CaO(g)\downarrow + 2NO_2 + O \quad (9)$$

$$Ca(NO_3)_2(l) \leftrightarrow CaO(g) + 2NO_2 + O \quad (10)$$

The calculated value, $\tau a \Delta_c H_T^0 / \nu$=84 kJ mol^{-1} [44], practically coincides with the experimentally obtained difference in parameters *E* for melted and solid nitrates, i.e., to 86 kJ mol^{-1}.

Thus, the decelerating influence of melting on the rate of reactant decomposition is in complete agreement with the CDV mechanism. It is doubtful that any other explanation of this unusual effect can be found within the framework of commonly accepted views.

Difference in the E parameters for the induction and acceleration periods (quantitative analysis)

This effect was observed for many reactants including some metal oxalates. The thermal decompositions of oxalates have been studied for more than 130 years [46]. Nevertheless, many features of these reactions remained unclear until recently. Among them was the significant difference in the parameters *E* for the induction and acceleration periods in the decompositions of $Ag_2C_2O_4$ and NiC_2O_4. This effect has been quantitatively interpreted by L'vov [13] within the framework of the CDV mechanism.

The difference in the parameters *E* for the induction and acceleration periods in the decomposition of $Ag_2C_2O_4$ and NiC_2O_4 is equal to 59 and 68 kJ mol^{-1} [47, 48], respectively. The calculated condensation energy per mole of products ($-\tau_1 a \Delta_c H_T^0 / \nu$) is equal to 63 kJ mol^{-1} for both reactants [13]. In these calculations: $-\Delta_c H_T^0$ is 284.9 and 428.8 kJ mol^{-1}, τ_1 is 0.50 and 0.51, *a* is 2 and 1, and ν is 4.5 and 3.5 (Table 1), respectively. The experimental and theoretical values are in close agreement. This proves the validity of the CDV mechanism once again.

Conclusions

Elementary thermochemical calculations show that in all cases of formation of solid product in the process of the congruent dissociative vaporization (CDV) of the reactants, the equilibrium partial pressure, P_{eqp}, of the main product greatly exceeds its saturation vapour pressure, such that the vapour oversaturation varies in the range from 10^3 to 10^{53}. It is remarkable that the CDV is the only chemical process, which is accompanied by the appearance of vapour oversaturation of the low-volatility product. There is no alternative to this simple and universal combination of fundamental importance (for the theory of solid decompositions). The average value of P_{eqp} at the induction stage is about $2 \cdot 10^{-17}$ bar for all 30 reactants under this study, and $1 \cdot 10^{-13}$ bar for all reactants except 11 hydroxides and hydrates. These pressures are enough for the formation of germ nuclei on the surface of the reactants. At the following acceleratory and deceleratory stages, owing to the transfer of condensation energy to the reactant in the reaction interface, the P_{eqp} value reaches and exceeds 10^{-9} bar.

A degree of vapour oversaturation is responsible for the amorphous or crystalline structure of the solid product and for the value of the condensation energy transfer. In turn, variations in the energy transfer explain two unexpected effects observed in the decomposition kinetics: the increase of the molar enthalpy with temperature and the decelerating influence of melting on the rate of decomposition.

In retrospect, the above fundamental features of decomposition kinetics might have been interpreted 70 years ago if the possibility of the congruent dissociative vaporization of a reactant as a primary stage of solid-state decompositions had not been rejected without any serious analysis. Thereafter the problem has been practically forgotten for years. A state of stagnation in the generally accepted theory established and appraised by Galwey and Brown [49] in 2000 remains without any forward progress up to now. Meanwhile, the CDV mechanism that explains the main peculiarities of decomposition kinetics re-

main unclaimed by the TA community even today, more than a decade after its thorough analysis and justification [50, 51].

Acknowledgements

The author thanks his grandson Nikita L'vov (Montreal, Canada) for the linguistic improvement of the manuscript of this paper.

References

1 M. Volmer, Kinetik der Phasenbildung, Steinkopff, Leipzig 1939.
2 W. J. Dunning, Chemistry of the Solid State, W. E. Garner, Ed., Butterworths, London 1955, Chapter 6.
3 J. P. Hirth and G. M. Pound, Condensation and Evaporation. Nucleation and Growth Kinetics, Pergamon Press, Oxford 1963.
3 H. Green and W. Lane, Particulate Clouds: Dusts, Smokes and Mists, London 1964.
5 J. F. Dettorre, T. G. Knorr and E. H. Hall, Vapor Deposition, C. F. Powell, J. H. Oxley and J. M. Blocher, Jr., Eds, Wiley, New York 1966, Chapter 3.
6 J. Zawadzki and S. Bretsnajder, Trans. Faraday Soc., 34 (1938) 951.
7 S. Z. Roginsky, Trans. Faraday Soc., 34 (1938) 959.
8 P. W. M. Jacobs and F. C. Tompkins, Chemistry of the Solid State, W. E. Garner, Ed., Butterworths, London 1955, Chapter 7.
9 M. E. Brown, D. Dollimore and A. K. Galwey, Reactions in the Solid State, Elsevier, Amsterdam 1980.
10 P. W. M. Jacobs, J. Phys. Chem., B 101 (1997) 10086.
11 B. V. L'vov, Spectrochim. Acta, Part B, 53 (1998) 809.
12 B. V. L'vov, Thermochim Acta, 315 (1998) 145.
13 B. V. L'vov, Thermal Decomposition of Solids and Melts. New Thermochemical Approach to the Mechanism, Kinetics and Methodology, Springer, Berlin 2007.
14 A. K. Galwey and G. M. Laverty, Solid State Ionics, 38 (1990) 155.
15 W. E. Garner, Chemistry of Solid State, Butterworths, London 1955, Chapter 8.
16 A. K. Galwey and M. E. Brown, Thermal Decomposition of Ionic Solids, Elsevier, Amsterdam 1999.
17 J. A. Cooper and W. E. Garner, Trans. Faraday Soc., 32 (1936) 1739.
18 A. K. Galwey, R. Spinicci and G. G. T. Guarini, Proc. Roy. Soc., A378 (1981) 477.
19 N. F. Mott, Proc. Roy. Soc., A172 (1939) 325.
20 A. K. Galwey, N. Koga and H. Tanaka, J. Chem. Soc. Faraday Trans., 86 (1990) 531.
21 M. E. Brown, A. K. Galwey, M. A. Mohamed and H. Tanaka, Thermochim. Acta, 235 (1994) 255.
22 B. Welz, G. Schlemmer, H. M. Ortner and W. Wegscheider, Prog. Anal. Spectrosc., 12 (1989) 111.
23 M. M. Dubinin, O. Kadlec and B. Ponec, Kinet. Katal., 8 (1967) 292.
24 A. N. Modestov, P. V. Poplaukhin and N. Z. Lyakhov, J. Therm. Anal. Cal., 65 (2001) 121.
25 V. Kohlschütter and H. Nitschmann, Z. Phys. Chem. Bodenstein Festband, (1931) 494.
26 M. Volmer and G. Seydel, Z. phys. Chem., A179 (1937) 153.
27 G. B. Frost, K. A. Moon and E. H. Tompkins, Can. J. Chem., 29 (1951) 605.
28 G. B. Frost and R. A. Campbell, Can. J. Chem., 31 (1953) 107.
29 H. W. Quinn, R. W. Missen and G. B. Frost, Can. J. Chem., 33 (1955) 286.
30 R. A. W. Haul and F. R. L. Schöning, Z. Anorg. Allg. Chem., 269 (1952) 120.
31 B. Liu, P. S. Thomas, A. S. Ray and J. P. Guerbois, J. Therm. Anal. Cal., 88 (2007) 145.
32 M. G. Kim, U. Dahmen and A. W. Searcy, J. Am. Ceram. Soc., 70 (1987) 146.
33 J. Ewing, D. Beruto and A. W. Searcy, J. Am. Ceram. Soc., 62 (1979) 580.
34 T. K. Basu and A. W. Searcy, J. Chem. Soc. Faraday Trans., I 72 (1976) 1889.
35 C. N. R. Rao, P. J. Thomas and G. U. Kulkarni, Nanocrystal: Properies and Applecations, Springer, Berlin 2007.
36 R. C. Jaeger, Film Deposition, Introduction to Microelectronic Fabrication, Prentice Hall, Upper Saddle River 2002.
37 B. V. L'vov, Evaporation, Thermal Dissociation, Carbothermal Reduction and Thermal Decomposition of Substances. A General Approach to the Theoretical Calculation of Kinetics, XXVII CSI, Bergen, Norway 1991, Book of Abstracts, A-5.2.
38 B. V. L'vov, Thermochim. Acta, 315 (1998) 145.
39 B. V. L'vov and V. L. Ugolkov, Thermochim. Acta, 411 (2004) 73.
40 B. V. L'vov and V. L. Ugolkov, Thermochim. Acta, 413 (2004) 7.
41 B. V. L'vov and V. L. Ugolkov, Thermochim. Acta, 401 (2003) 139.
42 B. V. L'vov and V. L. Ugolkov, J. Therm. Anal. Cal., 74 (2003) 697.
43 B. V. L'vov, J. Therm. Anal. Cal., 92 (2008) 639.
44 B. V. L'vov and V. L. Ugolkov, Thermochim. Acta, 424 (2004) 7.
45 C. Ettarh and A. K. Galwey, Thermochim. Acta, 288 (1996) 203.
46 B. V. L'vov, Thermochim. Acta, 364 (2000) 99.
47 J. Deren and R. Mania, Bull. Acad. Pol. Sci., 21 (1973) 387.
48 D. A. Dominey, H. Morley and D. A. Young, Trans. Faraday Soc., 61 (1965) 1246.
49 A. K. Galwey and M. E. Brown, J. Therm. Anal. Cal., 60 (2000) 863.
50 B. V. L'vov, Spectrochim. Acta, Part B, 63 (2008) 332.
51 B. V. L'vov, J. Therm. Anal. Cal., DOI: 10.1007/s10973-008-9372-9

Received: April 16, 2008
Accepted: October 14, 2008

DOI: 10.1007/s10973-008-9175-z